Role of Stargardt-3 macular dystrophy protein (ELOVL4) in the biosynthesis of very long chain fatty acids

Martin-Paul Agbaga*†, Richard S. Brush†‡, Md Nawajes A. Mandal†‡, Kimberly Henry†‡, Michael H. Elliott†‡, and Robert E. Anderson*†‡§

Departments of *Cell Biology and †Ophthalmology, University of Oklahoma Health Sciences Center and ‡Dean A. McGee Eye Institute, 608 Stanton L. Young Boulevard, Oklahoma City, OK 73104

Edited by John A. Glomset, University of Washington, Seattle, WA, and approved June 12, 2008 (received for review March 14, 2008)

Stargardt-like macular dystrophy (STGD3) is a dominantly inherited juvenile macular degeneration that eventually leads to loss of vision. Three independent mutations causing STGD3 have been identified in exon six of a gene named *Elongation of very long chain fatty acids 4* (*ELOVL4*). The ELOVL4 protein was predicted to be involved in fatty acid elongation, although evidence for this and the specific step(s) it may catalyze have remained elusive. Here, using a gain-of-function approach, we provide direct and compelling evidence that ELOVL4 is required for the synthesis of C28 and C30 saturated fatty acids (VLC-FA) and of C28-C38 very long chain polyunsaturated fatty acids (VLC-PUFA), the latter being uniquely expressed in retina, sperm, and brain. Rat neonatal cardiomyocytes and a human retinal epithelium cell line (ARPE-19) were transduced with recombinant adenovirus type 5 carrying mouse *Elovl4* and supplemented with 24:0, 20:5n3, or 22:5n3. The 24:0 was elongated to 28:0 and 30:0; 20:5n3 and 22:5n3 were elongated to a series of C28-C38 PUFA. Because retinal degeneration is the only known phenotype in STGD3 disease, we propose that reduced VLC-PUFA in the retinas of these patients may be the cause of photoreceptor cell death.

fatty acid biosynthesis | macular degeneration

Three independent mutations in the last exon (exon-VI) of the *ELOVL4* gene are associated with dominant Stargardt-like macular dystrophy (STGD3) in humans (1–4). These mutations cause a frame-shift that introduces a stop codon, resulting in premature termination of the protein and removal of the signal sequence for targeting the protein to its putative cellular location, the endoplasmic reticulum (1, 4). As a result, the mutant protein mis-localizes and aggregates (3, 5, 6), and, when coexpressed with the wild type protein, the mutant and wild-type proteins associate and mis-localize (3, 7). Based on sequence homology with a group of functional yeast genes and other mammalian *ELOVLs*, the ELOVL4 protein was predicted to be involved in elongation of very long chain fatty acids (1, 5, 8). For example, the yeast microsomal Elo1p is responsible for elongation of carbon chains between 14:0 and 16:0 (9). Yeast Elo2p and Elo3p, and mammalian ELOVL1, 2, 3, and 5 have been shown to be involved in elongation of saturated, monounsaturated, or polyunsaturated fatty acids (PUFA) from 18 to 26 carbons (10–12). However, a role for ELOVL4 protein in fatty acid elongation and the specific step(s) it may catalyze have remained elusive (13, 14). Based on the abundant expression of ELOVL4 protein in photoreceptor cells of the retina (15–17) and to lesser extents in brain, testis, and skin (17), it was first hypothesized that ELOVL4 may be involved in the biosynthetic pathway of docosahexaenoic acid (22:6n3, DHA), the most abundant PUFA in the retina and the brain (1, 16, 18). A series of experiments carried out in our laboratory (unpublished data) does not support this hypothesis.

Recent reports establish ELOVL4 as an essential protein for growth and development, as neonatal lethality is observed in both homozygous *Elovl4* knockout and knockin mouse models (19–22). Heterozygous knockin animals carrying a mutant mouse gene, a condition similar to human STGD3, showed slow but significant changes in retinal morphology (23), accumulation of lipofuscin (23), and altered visual function (22, 23). Also, transgenic mice expressing the mutant form of human *ELOVL4* that causes STGD3 accumulate undigested phagosomes and lipofuscin-derived fluorophores in the retinal pigment epithelium (RPE), followed by RPE atrophy and subsequent photoreceptor degeneration in the central retina (4), as observed in human dominant STGD3 (1, 24), recessive Stargardt disease (25), and age-related macular degeneration (26, 27). Furthermore, homozygous *Elovl4* knockout and knockin neonates, which died within hours of birth, exhibited scaly wrinkled skin and a severely compromised epidermal permeability barrier, most likely resulting from a global reduction in very long chain saturated and monounsaturated fatty acids (VLC-FA, chain length ≥26:0) in both omega hydroxyl ceramides/glucosylceramides and free fatty acids (19–22).

To establish the specific step(s) that the ELOVL4 protein catalyzes in very long chain fatty acid elongation, we overexpressed transgenic ELOVL4 protein in rat neonatal cardiomyocytes and a human RPE cell line (ARPE-19), neither of which express detectable levels of endogenous ELOVL4 protein, and treated them with several fatty acid precursors. Results obtained by gas chromatography-mass spectrometry (GC-MS) show that ELOVL4 protein is indeed a component of a fatty acid elongation system that catalyzes synthesis of 28:0 and 30:0 VLC-FA and of C28-C38 VLC-PUFA, the latter being uniquely found in retina (28, 29), sperm (29, 30), and brain (31). We propose that these steps are important in these tissues for the local synthesis of VLC-PUFA (C28-C36) that are esterified into phosphatidylcholine in rod outer segment membranes and brain, or amide-bound into sphingolipids and ceramides in germ cells (32) and sperm of some mammals (33).

Results

To establish the role of ELOVL4 in fatty acid elongation and to identify the specific step in which it may be involved, we

Author contributions: M.-P.A., R.S.B., M.N.A.M., M.H.E., and R.E.A. designed research; M.-P.A., R.S.B., M.N.A.M., K.H., and M.H.E. performed research; M.-P.A. and R.S.B. contributed new reagents/analytic tools; M.-P.A., R.S.B., M.N.A.M., M.H.E., and R.E.A. analyzed data; and M.-P.A., R.S.B., M.N.A.M., M.H.E., and R.E.A. wrote the paper.

Conflict of interest statement: M.-P.A., R.S.B., and R.E.A. have filed a provisional patent for the use of very long chain polyunsaturated fatty acids in the treatment of macular degeneration.

This article is a PNAS Direct Submission.

Freely available online through the PNAS open access option.

§To whom correspondence should be addressed. E-mail: robert-anderson@ouhsc.edu.

This article contains supporting information online at www.pnas.org/cgi/content/full/0802607105/DCSupplemental.

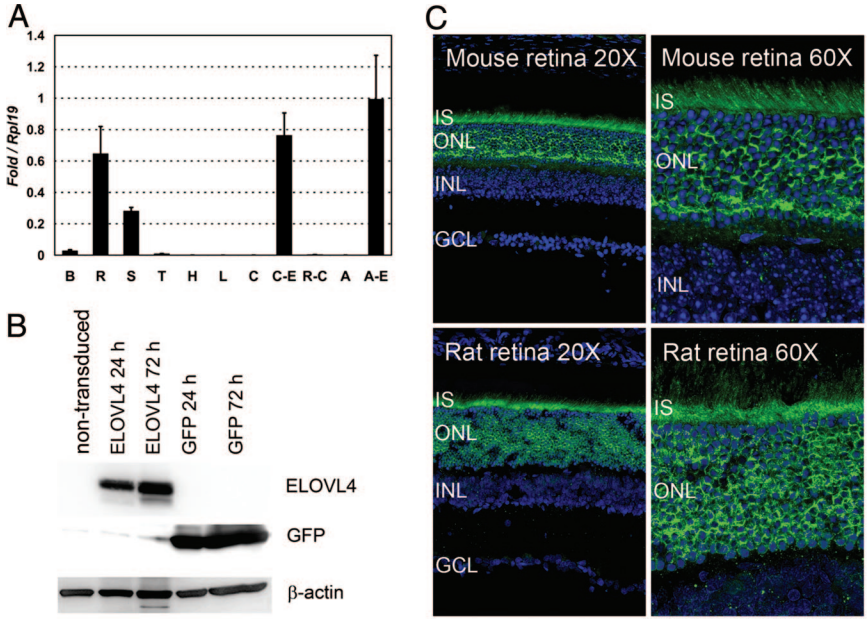

Fig. 1. Transgenic expression of mouse *ELOVL4* in rat cardiomyocytes and ARPE-19 cells. (*A*) Comparison of quantitative expression of *Elovl4* gene in different rat tissues and in ARPE-19 cells by qRT-PCR, and presented relative to the expression of the housekeeping gene *Rpl 19*. The values represent the means (± SEM) of $n = 3$ after normalizing with *Rpl 19* calculated by the comparative threshold cycle (C_t) method. Significant expression of *Elovl4* was observed in transduced cells. B, brain; R, retina; S, skin; T, testis; H, heart; L, liver; C, cardiomyocytes; C-E, *Elovl4*-expressing cardiomyocytes; R-C, RPE-Choroid; A, ARPE-19; A-E, *Elovl4*-expressing ARPE-19 cells. (*B*) Western blots showing expression of ELOVL4, GFP, and β-actin in cardiomyocytes transduced with or without recombinant adenoviruses. The nontransduced and GFP-expressing controls did not show ELOVL4 expression, whereas *Elovl4*-transduced cells showed abundant ELOVL4 protein expression. (*C*) ELOVL4 immunolabeling is detected in mouse and rat retinas, using affinity-purified ELOVL4 antibodies (green). Nuclei were stained with 4′,6-diamidino-2-phenylindole (blue). Images were captured by using an Olympus FluoView Confocal Microscope with 20× and 60× objective lenses. IS, inner segments of rod and cone photoreceptors; ONL, outer nuclear layer; INL, inner nuclear layer; GCL, ganglion cells layer.

expressed mouse *Elovl4* in rat neonatal cardiomyocytes and in human ARPE-19 cells, neither of which express significant levels of ELOVL4 mRNA as measured by quantitative real-time PCR (qRT-PCR) (Fig. 1*A*). The highest endogenous level of *Elovl4* expression was detected in rat retina and skin (Fig. 1*A*). Brain and testis also showed significant levels of expression, which were 1/20 and 1/70 of the retina, respectively. Liver, heart, and cultured cardiomyocytes showed negligible levels of expression, corresponding well with previous observations in mice (17). In cultured rat cardiomyocytes, endogenous *Elovl4* expression was ≈1/2,500 of that found in the retina (Fig. 1*A*). However, when transduced with adenovirus carrying mouse *Elovl4*, the expression levels in cardiomyocytes and ARPE-19 cells increased 1,000 to 3,000-fold compared with nontransduced cells and were comparable to those observed in rat retina (Fig. 1*A*). Transduction efficiency in both cell types was >90% as determined by immunocytochemistry (data not shown). Expression of ELOVL4 protein in transduced cells was confirmed by Western blot analysis (Fig. 1*B*) using a specific antibody that recognizes both mouse and rat ELOVL4 [supporting information (SI) Fig. S1]. ELOVL4 was not detected in control cells (nontransduced and *GFP*-transduced cells) but was abundant in cardiomyocytes (Fig. 1*B*) and ARPE-19 cells (data not shown) transduced with *Elovl4*. Immunohistochemical localization in rat and mouse retinas showed that ELOVL4 is confined to photoreceptor inner segments and to the cytoplasm surrounding photoreceptor nuclei (Fig. 1*C*), consistent with the reported localization of ELOVL4 protein (3, 16).

We then tested whether expression of ELOVL4 can lead to elongation of the saturated long chain fatty acid lignoceric acid (24:0), a precursor of VLC-FA (34, 35). From the fatty acid methyl ester (FAME) data obtained by GC-MS, we found that cardiomyocytes and ARPE-19 cells, irrespective of ELOVL4 overexpression, were able to internalize 24:0 and elongate it to 26:0 (Fig. 2). This elongation step is probably catalyzed by other endogenously expressed elongases (14, 36). However, VLC-FA elongation products beyond 26:0 were detected only in *Elovl4*-transduced cells (Fig. 2). The *Elovl4*-transduced cells showed significant elongation of 26:0 to 28:0 relative to the two controls (79% increase in cardiomyocytes compared with 11% and 9% in control cells) (Fig. 2*B*). In ARPE-19, there was a 77% increase in 28:0 compared with 11% and 12% in the control cells (Fig. 2*D*). The 28:0 was further elongated to 30:0 in both cell types expressing ELOVL4. From these experiments, we conclude that ELOVL4 is necessary for the conversion of 26:0 to 28:0 and probably of 28:0 to 30:0. Because these fatty acids are incorporated into sphingolipids and ceramides, our findings support earlier results in which deletion of *Elovl4* in mice resulted in reduced VLC-FA levels in skin and neonatal lethality because of defects in skin barrier permeability (19–21).

In the retina, sphingolipids and ceramides are minor components of the lipid pool (18). Instead, n3 and n6 VLC-PUFA are esterified into phosphatidylcholine molecular species (28) that have been shown to interact with rhodopsin (37), the major phototransduction protein in the retina. These VLC-PUFA can be synthesized from long chain polyunsaturated fatty acid (LC-PUFA) precursors in the retina, although the elongase(s) responsible for their biosynthesis has never been identified (38). Therefore, we hypothesized that ELOVL4 may play a role in biosynthesis of the VLC-PUFA found in the retina, brain, and sperm.

To test this hypothesis, we examined the ability of *Elovl4*-transduced cardiomyocytes to elongate the VLC-PUFA precursors eicosapentaenoic acid (20:5n3) and docosapentaenoic acid (22:5n3). *Elovl4*- or *GFP*-transduced and nontransduced cardiomyocytes treated with 20:5n3 or 22:5n3 for 48 h or 72 h elongated both precursors to C24 and C26 n3 PUFA, independent of transgene expression (Fig. 3). However, *Elovl4*-

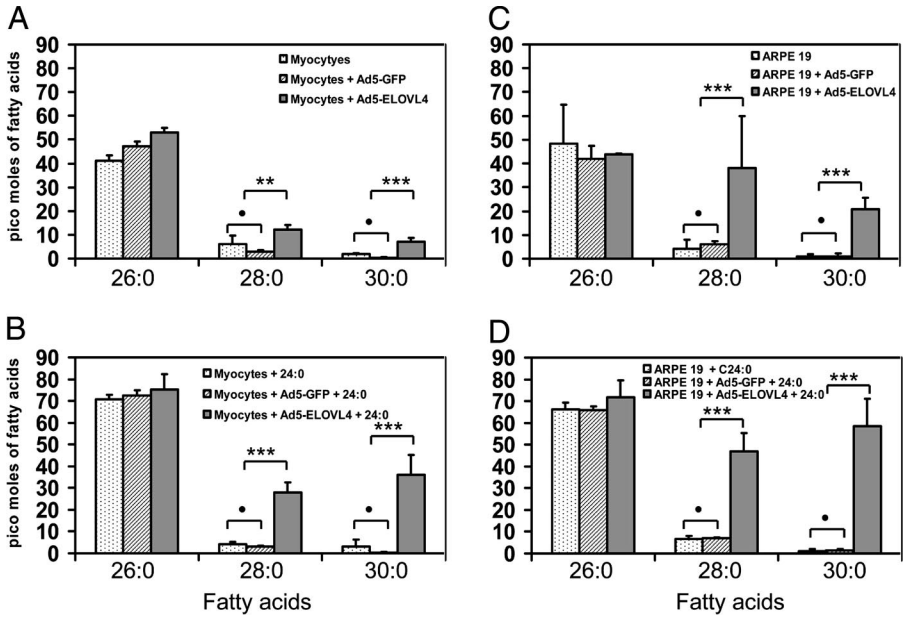

Fig. 2. Biosynthesis of 28:0 and 30:0 from 24:0 in cardiomyocytes and ARPE-19 cells expressing *Elovl4* transgene. Cardiomyocytes or ARPE-19 cells were transduced with or without recombinant *Elovl4* or *GFP* viruses for 24 h and then cultured in 24:0-supplemented complete media for 72 h. Total lipids extracted from an aliquot of homogenate equivalent to 500 μg of protein were converted to FAME and analyzed by GC-MS in the SIM mode. (*A* and *B*) Cardiomyocytes without (*A*) and with (*B*) 24:0. (*C* and *D*) ARPE-19 cells without (*C*) and with (*D*) 24:0. The 26:0, 28:0 and 30:0 response values were obtained by using the *m/z* ratios 410.4, 438.4, and 466.5, respectively. Sample concentrations were determined by comparison to external standards, using 25:0 and 27:0 as internal standards. Multivariate ANOVA with posthoc Scheffé test was used to determine statistical significance. ●, no significant difference; **, $P < 0.01$; ***, $P < 0.001$ ($n = 3$).

transduced cells, but not the controls, further elongated each of these precursors to 28:5n3, 30:5n3, 32:5n3, 34:5n3, 36:5n3, and 38:5n3 (Fig. 3 *B* and *C*). In the *Elovl4*-transduced cells, the major VLC-PUFA products were 34:5n3 and 36:5n3. In addition, 34:6n3 and 36:6n3, products of desaturase activity, were also generated, probably by the pathways shown in Fig. 4. Identification and confirmation of each of the VLC-PUFA peaks on the chromatogram are described in Figs. S2 and S3.

We suggest that ELOVL4 protein is a component of an elongase system necessary for the biosynthesis of VLC-PUFA (beyond C26) that are incorporated into ceramides, sphingomyelin, and the *sn-1* position of phosphatidylcholine, an activity that has not been established (28, 29, 37). To explore this possibility, we separated total lipids from 20:5n3-treated *Elovl4*-transduced cells into individual lipid classes by two-dimensional thin layer chromatography (39) and analyzed the FAME from each class by GC-MS. The VLC-PUFA synthesized by ELOVL4 were present in these three complex lipids and in the free fatty acid pool (Fig. S4). There were no detectable VLC-PUFA in phosphatidylinositol, phosphatidylethanolamine, or phosphatidlyserine (data not shown).

Discussion

Previous studies established that the ELO family of proteins comprises enzymes involved in fatty acid elongation (8, 12, 14). Mammalian ELOVLs that share similar specific conserved motifs with ELOVL4, such as the dilysine endoplasmic reticulum (ER) retention motif (KXKXX) and a conserved histidine-rich motif (HXXHH) believed to act as an iron-chelating ligand used for electron transfer for O_2-dependent redox reactions, are also involved in fatty acid biosynthesis (3, 40). Our findings establish ELOVL4 as a component of an elongation system for both saturated and polyunsaturated fatty acids. We propose that ELOVL4 is involved in very long chain fatty acid biosynthesis and specifically elongates both saturated and unsaturated C26 to C28 products (Fig. 4). Given the absence of further elongation without the expression of ELOVL4, we suggest that this enzyme also catalyzes the elongation of C28 to C30-C38 products. However, final proof of its involvement in these subsequent elongation steps will come when specific C28–C36 precursor fatty acids become available for testing. It is interesting in this elongation scheme that 20:5n3 and 22:5n3, but not 22:6n3, are predicted precursors of VLC-PUFA (Fig. 4). When bovine retinas were incubated with either [^{14}C]-22:5n3 or [^{14}C]-22:6n3, 22:5n-3 was selectively converted to 24:5n3, whereas 22:6n3 was not (41). Furthermore, when retinas were incubated with [^{14}C]-acetate, radioactivity accumulated in 24:5n3 and was further incorporated into fatty acids with chain lengths up to 36 carbons, indicating the retina as the site of elongation of VLC-PUFA (41). Similarly, after intravitreal injection of radiolabeled 20:5n3 and 22:6n3, only 20:5n3 was incorporated to any extent into the VLC-PUFA (38).

Although STGD3 is an autosomal dominant disease, it is expressed in the retina as a loss of function because the mutated product, a truncated protein, acts in a dominant negative manner by binding and dimerizing with the wild type protein, which most likely leads to loss of enzymatic activity (3, 6, 7). In support of this suggestion are recent reports (42, 43) that mice heterozygous for *Elovl4* expression do not have retinal degeneration or loss of function, leading the authors to conclude that the pathology in STGD3 is not due to haploinsufficiency. Because the ELOVL4 protein is required for the synthesis of both VLC-FA and VLC-PUFA but expression of the STGD3 phenotype is only in the retina and not in the skin, we suggest that the pathology in the retina results from the loss of VLC-PUFA rather than VLC-FA.

The function of VLC-PUFA in the retina or in any tissue is largely unknown. Their synthesis in retina, brain, and testis but not liver (which lacks ELOVL4 expression) indicates that VLC-PUFA are synthesized locally in these tissues (38, 41, 44, 45). Also, VLC-FA, which we have also shown to be synthesized by ELOVL4 (Fig. 2), are abundant in skin ceramides (19–22). Thus, the tissues that can locally synthesize or are abundant in VLC-PUFA and/or VLC-FA are the same tissues with the highest

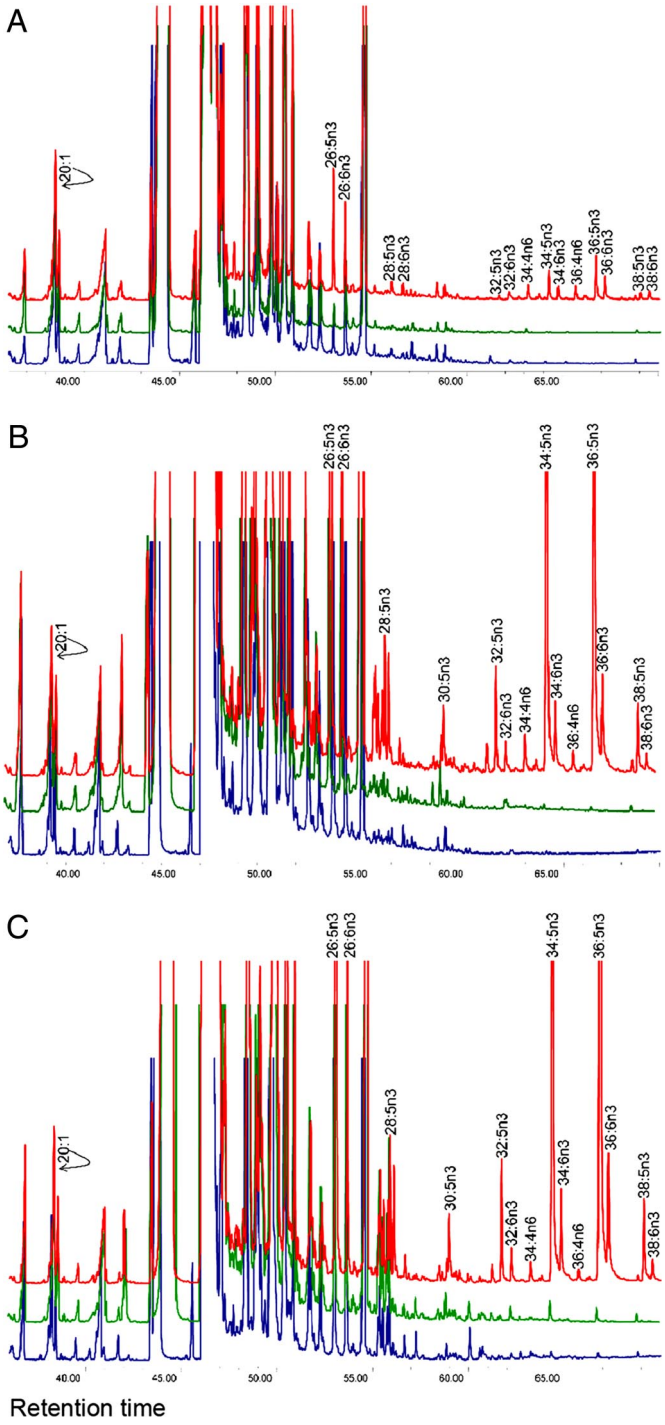

Fig. 3. Biosynthesis of VLC-PUFA in cardiomyocytes expressing *Elovl4* transgene. GC-MS allowed identification of the VLC-PUFA derived from sample equivalent to 2.0 mg of protein from cardiomyocytes treated with 20:5n3 or 22:5n3 for 72 h after transduction with recombinant *Elovl4* or *GFP* viruses for 24 h ($n = 3$). The PUFA response values were obtained by using the *m/z* ratios 79.1, 108.1, and 150.1 in SIM mode and abundances were compared by normalizing the chromatograms to the response of 20:1. (*A*) Rat cardiomyocytes expressing *ELOVL4* (red) or *GFP* (green) and nontransduced cells (blue) were cultured without precursors for 72 h. All cells, irrespective of ELOVL4 expression, synthesized C22-C26 PUFA. ELOVL4 expression in the absence of precursors resulted in elongation of endogenous precursor to C28-C38 VLC-PUFA. (*B*) Cardiomyocytes in *A* above cultured with 20:5n3 synthesized C24-C26 in all treatment groups. Significant biosynthesis of C28-C38 n3 VLC-PUFA occurred in *Elovl4*-transduced cells (red), but not in *GFP* (green) and nontransduced cells (blue), with accumulation of 34:5n3 and 36:5n3. (*C*) Cardiomyocytes in *A* above cultured with 22:5n3 synthesized C24-C26 in all treatment groups. They also synthesized the same n3 VLC-PUFA as found for 20:5n3. Note that each chromatogram was normalized to endogenous 20:1, which did not change among the sample groups.

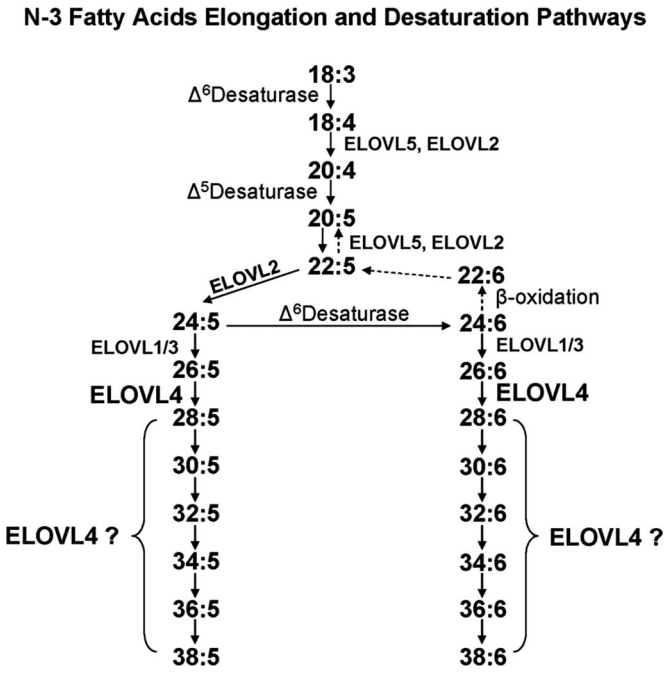

Fig. 4. Schematic diagram of *in vivo* n3 VLC-PUFA biosynthetic pathway mediated by ELOVL4 and other ELO families [modified after Suh and Clandinin (38)]. 18:3n3, 20:5n3, or 22:5n3 can be converted to VLC-PUFA through consecutive enzymatic activities of desaturases and elongases. Although some elongases are specific for a single step, others are nonspecific or multifunctional and act at several steps (e.g., human ELOVL5 and murine ELOVL2) (11). We propose that ELOVL4 is essential for elongation of saturated 26:0 to 28:0 and of 26:5n3 to 28:5n3. It is also possible that ELOVL4 is necessary for generating (C30–C38):5n3 because these fatty acids are formed only in ELOVL4 expressing cells. However, other ELOVLs may be responsible for elongations of some of these VLC-PUFA (C30–C38) by using products generated by ELOVL4 elongase activity. The synthesis of 34:6n3 and 36:6n3 in our study suggests desaturase activity on their shorter chain precursors. However, the specific desaturase(s) involved is not known.

levels of *Elovl4* expression (Fig. 1*A*). We have shown that expression of ELOVL4 in cells that do not normally express the protein confers on them the ability to synthesize VLC-PUFA and VLC-FA from shorter chain precursors that are present in tissues expressing ELOVL4. Based on this result and the studies in refs. 38, 41, 44, and 45, we conclude that ELOVL4 plays a major role in the local biosynthesis of VLC-PUFA in the retina, brain, and testis in biosynthesis of VLC-FA found in the skin.

Because of their great length and minor abundance, which makes them difficult to analyze, VLC-PUFA have been largely ignored since their discovery >20 years ago (28, 31). However, because of their unusually long hydrocarbon chains (>C26), the proximal end of which resembles a saturated fatty acid and the distal end a PUFA, they may play important roles in biological systems that cannot be replaced by the more common shorter chain fatty acids (C16-C18) or even the C20-C22 PUFA (46). By their structure, some are able to span and reside within both leaflets of the lipid bilayer, thereby giving stability to highly curved cellular membranes such as surrounding nuclear pore complexes (47) or, putatively, the rims of photoreceptor disk membranes and sperm heads. It was recently reported that

retinas of STGD3 knockin mice that carry the human pathogenic 5-bp deletion in the mouse *Elovl4* gene have reduced levels of C32-C36 acyl phosphatidylcholines and altered retinal function (48). Thus, it seems reasonable to suggest that significant reduction of these VLC-PUFA, which may be necessary for normal retinal function, may contribute to Stargardt-3 macular dystrophy.

In summary, we have shown that ELOVL4 is necessary for synthesis of VLC-FA and VLC-PUFA, the latter of which are mainly present in retinal outer segment membranes in phosphatidylcholine. This unique class of phospholipids, which contains VLC-PUFA in the *sn-1* position and 22:6n3 in the *sn-2* position (37), may be necessary for normal function of the retina, and their absence or reduction may cause photoreceptor degeneration seen in STGD3 patients.

Materials and Methods

Construction of Recombinant Adenovirus Carrying Mouse ELOVL4. Recombinant adenovirus carrying the *mouse Elovl4* gene was constructed by using Adeno X Expression Systems 2 with creator technology protocols (Clontech). Briefly, the *Elovl4* cDNA (from the translation start codon to the termination codon) was cloned in frame with the lox P site of the pDNR-CMV donor vector. The purified donor plasmid was sequenced and ELOVL4 protein expression verified by Western blot analysis after transfection of the plasmid into HEK 293 cells. Cre-lox recombination reaction was carried out to transfer the cloned *Elovl4* cDNA to the pLp-Adeno-X CMV Adenovirus type 5 acceptor backbone, which places the *Elovl4* cDNA under the control of the CMV promoter. Recombinants were selected, sequenced, confirmed, purified, and digested with PacI and then transfected into HEK 293 cells to generate virus particles. The recombinant viruses were prepared as high-titer stocks through the propagation in HEK 293 cells by double cesium chloride purification, and dialyzed against a 10 mM Tris (pH 8.0) buffer that contained 80 mM NaCl, 2 mM $MgCl_2$, and 10% glycerol (49). Infectious adenovirus titer was determined in triplicate by plaque-forming assay and expressed as plaque-forming units (pfu) per ml.

Cell Culture. Rat neonatal cardiomyocytes were isolated from 1- or 2-day-old rats, using the National Cardiomyocyte Isolation System (Worthington). The isolated cells (5×10^6) were plated in 10-cm tissue culture plates and cultured in DMEM:F-12 (1:1) medium containing 10% (vol/vol) FBS and 5% (vol/vol) horse serum supplemented with sodium pyruvate (1 mM), penicillin (100 units/ml), and streptomycin (100 units/ml) at 37°C in a tissue culture incubator with constant supply of 5% CO_2 in 95% relative humidity. Cells were used for experiments after 2–3 days in culture. ARPE-19 cells (2×10^6) were cultured under the same conditions as cardiomyocytes.

Adenovirus infections of cardiomyocytes and ARPE-19 cells were carried out as described in refs. 50 and 51. After 24 h of incubation, the infection medium was replaced with normal [15% (vol/vol) serum] culture medium supplemented separately with either 50 or 100 μg/ml of the sodium salt of 24:0 or either 30 or 50 μg/ml of 20:5n3 or 22:5n3 (conjugated to BSA fraction V) (34). After incubation with these fatty acids for 48 or 72 h, cells were washed in PBS containing 50 μM fatty acid free BSA fraction V and then washed twice more with only PBS. They were then scraped and stored as pellets at −80°C until used.

Production and Characterization of Affinity-Purified ELOVL4 Antibodies. A synthetic 12-amino acid peptide corresponding to amino acids 301–312 of the mouse ELOVL4 protein was conjugated to keyhole limpet hemocyanin and injected s.c. into rabbits for polyclonal antibody production after collection of preimmune serum. Affinity-purified antibodies were collected by using immobilized peptide antigen (Bethyl Laboratory). The affinity-purified antibody specificity was determined by Western blot analysis on HEK 293 cells transfected with mouse *Elovl4* and on lysates from mouse and rat retinas, brain, and skin and on bovine retina lysates. On 10% or 12% polyacrylamide gels, the antibody recognizes an ≈32-kDa protein, which was specifically blocked by preincubation of the antibody with the antigenic peptide (Fig. S1). This size is similar to that reported by Grayson and Molday (3) for the human ELOVL4 protein. The antibody also showed intense labeling of ELOVL4 protein in the inner segment and the perinuclear region of the outer nuclear layer of mouse and rat retinas (Fig. 1*C*) in agreement with the localization reported in human retina (3) and other mammalian retinas (16) and was specifically blocked by the peptide (data not shown). Immunocytochemistry, Western blot analysis, and details of lipid extractions and analyses are described in detail in *SI Text*.

FAME Analysis by GC-MS. Fatty acid methyl esters were identified and quantified by using an Agilent Technologies 6890N gas chromatograph (GC) with a 5975B inert XL mass spectrometer (MS) detector (Agilent Technologies). The GC-MS was operated in the electron impact (EI) single ion monitoring (SIM) mode. For VLC-FA analysis, the injection volume was 1 μl and the inlet, held at 320°C, was set to pulsed splitless mode. An Agilent Technologies HP-5ms column (30 m × 0.25 mm × 0.25 μm) was used with a helium carrier gas flow rate of 1.2 ml/min. The oven temperature began at 160°C, was ramped to 320°C at 3°C/min, and was held at 320°C for 20 min. The MS transfer line, ion source, and quadrupole temperatures were 320°C, 230°C, and 150°C, respectively. The 26:0, 28:0, and 30:0 response values were obtained by using the *m/z* ratios 410.4, 438.4, and 466.5, respectively. Sample concentrations were determined by comparison to external standards, using 25:0 and 27:0 as internal standards. Multivariate ANOVA with post hoc Scheffé tests determined statistical significance ($P < 0.05$).

For VLC-PUFA analysis, the injection volume was 1 μl and the inlet, held at 290°C, was set to pulsed splitless mode. An SGE BPX70 column (35 m × 0.22 mm × 0.25 μm) was used with a helium carrier gas flow rate of 1.2 ml/min. The oven temperature began at 90°C for 10 min, was ramped to 290°C at 3°C/min, and was held at 290°C for 12.3 min. The MS transfer line, ion source, and quadrupole temperatures were 290°C, 230°C, and 150°C, respectively. The PUFA response values were obtained by using the *m/z* ratios 79.1, 108.1, and 150.1 in SIM mode. Comparisons were made by normalizing the chromatograms, using the response of 20:1.

ACKNOWLEDGMENTS. We thank Roger Astley (Dean A. McGee Eye Institute, Oklahoma City, OK) for assistance with virus purification and titer and Radha Ayyagari and Vidyullatha Vasireddy (Shiley Eye Center, University of California, San Diego, CA) for initial discussions. This work was supported by National Eye Institute Grants EY04149, EY00871, and EY12190; National Center for Research Resources Grant RR17703; Research to Prevent Blindness, Inc.; and the Foundation Fighting Blindness.

1. Zhang K, *et al.* (2001) A 5-bp deletion in ELOVL4 is associated with two related forms of autosomal dominant macular dystrophy. *Nat Genet* 27:89–93.
2. Edwards AO, Donoso LA, Ritter R, III (2001) A novel gene for autosomal dominant Stargardt-like macular dystrophy with homology to the SUR4 protein family. *Invest Ophthalmol Vis Sci.* 42:2652–2663.
3. Grayson C, Molday RS (2005) Dominant negative mechanism underlies autosomal dominant Stargardt-like macular dystrophy linked to mutations in ELOVL4. *J Biol Chem* 280:32521–32530.
4. Karan G, *et al.* (2005) Lipofuscin accumulation, abnormal electrophysiology, and photoreceptor degeneration in mutant ELOVL4 transgenic mice: A model for macular degeneration. *Proc Natl Acad Sci USA* 102:4164–4169.
5. Ambasudhan R, *et al.* (2004) Atrophic macular degeneration mutations in ELOVL4 result in the intracellular misrouting of the protein. *Genomics* 83:615–625.
6. Karan G, *et al.* (2005) Loss of ER retention and sequestration of the wild-type ELOVL4 by Stargardt disease dominant negative mutants. *Mol Vis* 11:657–664.
7. Vasireddy V, *et al.* (2005) Stargardt-like macular dystrophy protein ELOVL4 exerts a dominant negative effect by recruiting wild-type protein into aggresomes. *Mol Vis* 11:665–676.
8. Tvrdik P, *et al.* (2000) Role of a new mammalian gene family in the biosynthesis of very long chain fatty acids and sphingolipids. *J Cell Biol* 149:707–718.
9. Schneiter R, Tatzer V, Gogg G, Leitner E, Kohlwein SD (2000) Elo1p-dependent carboxy-terminal elongation of C14:1Delta(9) to C16:1Delta(11) fatty acids in Saccharomyces cerevisiae. *J Bacteriol* 182:3655–3660.
10. Oh CS, Toke DA, Mandala S, Martin CE (1997) ELO2 and ELO3, homologues of the Saccharomyces cerevisiae ELO1 gene, function in fatty acid elongation and are required for sphingolipid formation. *J Biol Chem* 272:17376–17384.
11. Meyer A, *et al.* (2004) Novel fatty acid elongases and their use for the reconstitution of docosahexaenoic acid biosynthesis. *J Lipid Res* 45:1899–1909.
12. Westerberg R, *et al.* (2004) Role for ELOVL3 and fatty acid chain length in development of hair and skin function. *J Biol Chem* 279:5621–5629.
13. Leonard AE, Pereira SL, Sprecher H, Huang YS (2004) Elongation of long-chain fatty acids. *Prog Lipid Res* 43:36–54.
14. Jakobsson A, Westerberg R, Jacobsson A (2006) Fatty acid elongases in mammals: Their regulation and roles in metabolism. *Prog Lipid Res* 45:237–249.
15. Zhang XM, *et al.* (2003) Elovl4 mRNA distribution in the developing mouse retina and phylogenetic conservation of Elovl4 genes. *Mol Vis* 9:301–307.
16. Lagali PS, *et al.* (2003) Evolutionarily conserved ELOVL4 gene expression in the vertebrate retina. *Invest Ophthalmol Vis Sci* 44:2841–2850.
17. Mandal MN, *et al.* (2004) Characterization of mouse orthologue of ELOVL4: Genomic organization and spatial and temporal expression. *Genomics* 83:626–635.
18. Fliesler SJ, Anderson RE (1983) Chemistry and metabolism of lipids in the vertebrate retina. *Prog Lipid Res* 22:79–131.
19. Vasireddy V, *et al.* (2007) Loss of functional ELOVL4 depletes very long-chain fatty acids (> or =C28) and the unique omega-O-acylceramides in skin leading to neonatal death. *Hum Mol Genet* 16:471–482.

20. Cameron DJ, *et al.* (2007) Essential role of Elovl4 in very long chain fatty acid synthesis, skin permeability barrier function, and neonatal survival. *Int J Biol Sci* 3:111–119.
21. Li W, *et al.* (2007) Depletion of ceramides with very long chain fatty acids causes defective skin permeability barrier function, and neonatal lethality in ELOVL4 deficient mice. *Int J Biol Sci* 3:120–128.
22. McMahon A, *et al* (2007) Retinal pathology and skin barrier defect in mice carrying a Stargardt disease-3 mutation in elongase of very long chain fatty acids-4. *Mol Vis* 13:258–272.
23. Vasireddy V, *et al.* (2006) Elovl4 5-bp-deletion knock-in mice develop progressive photoreceptor degeneration. *Invest Ophthalmol Vis Sci* 47:4558–4568.
24. Edwards AO, *et al.* (1999) Autosomal dominant Stargardt-like macular dystrophy: I. Clinical characterization, longitudinal follow-up, and evidence for a common ancestry in families linked to chromosome 6q14. *Am J Ophthalmol* 127:426–435.
25. Allikmets R, *et al.* (1997) Mutation of the Stargardt disease gene (ABCR) in age-related macular degeneration. *Science* 277:1805–1807.
26. Zarbin MA (2004) Current concepts in the pathogenesis of age-related macular degeneration. *Arch Ophthalmol* 122:598–614.
27. Marx J (2006) Genetics. A clearer view of macular degeneration. *Science* 311:1704–1705.
28. Aveldano MI (1987) A novel group of very long chain polyenoic fatty acids in dipolyunsaturated phosphatidylcholines from vertebrate retina. *J Biol Chem* 262:1172–1179.
29. Aveldano MI (1992) Long and very long polyunsaturated fatty acids of retina and spermatozoa: The whole complement of polyenoic fatty acid series. *Adv Exp Med Biol* 318:231–242.
30. Poulos A, Sharp P, Johnson D, White I, Fellenberg A (1986) The occurrence of polyenoic fatty acids with greater than 22 carbon atoms in mammalian spermatozoa. *Biochem J* 240:891–895.
31. Poulos A, *et al.* (1986) Detection of a homologous series of C26–C38 polyenoic fatty acids in the brain of patients without peroxisomes (Zellweger's syndrome). *Biochem J* 235:607–610.
32. Furland NE, Zanetti SR, Oresti GM, Maldonado EN, Aveldano MI (2007) Ceramides and sphingomyelins with high proportions of very long-chain polyunsaturated fatty acids in mammalian germ cells. *J Biol Chem* 282:18141–18150.
33. Furland NE, *et al.* (2007) Very long-chain polyunsaturated fatty acids are the major acyl groups of sphingomyelins and ceramides in the head of mammalian spermatozoa. *J Biol Chem* 282:18151–18161.
34. Street JM, Johnson DW, Singh H, Poulos A (1989) Metabolism of saturated and polyunsaturated fatty acids by normal and Zellweger syndrome skin fibroblasts. *Biochem J* 260:647–655.
35. Street JM, Singh H, Poulos A (1990) Metabolism of saturated and polyunsaturated very-long-chain fatty acids in fibroblasts from patients with defects in peroxisomal beta-oxidation. *Biochem J* 269:671–677.
36. Westerberg R, *et al.* (2006) ELOVL3 is an important component for early onset of lipid recruitment in brown adipose tissue. *J Biol Chem* 281:4958–4968.
37. Aveldano MI (1988) Phospholipid species containing long and very long polyenoic fatty acids remain with rhodopsin after hexane extraction of photoreceptor membranes. *Biochemistry* 27:1229–1239.
38. Suh M, Clandinin MT (2005) 20:5n-3 but not 22:6n-3 is a preferred substrate for synthesis of n-3 very-long- chain fatty acids (C24–C36) in retina. *Curr Eye Res* 30:959–968.
39. Martin RE, Elliott MH, Brush RS, Anderson RE (2005) Detailed characterization of the lipid composition of detergent-resistant membranes from photoreceptor rod outer segment membranes. *Invest Ophthalmol Vis Sci* 46:1147–1154.
40. Chertemps T, *et al.* (2007) A female-biased expressed elongase involved in long-chain hydrocarbon biosynthesis and courtship behavior in Drosophila melanogaster. *Proc Natl Acad Sci USA* 104:4273–4278.
41. Rotstein NP, Pennacchiotti GL, Sprecher H, Aveldano MI (1996) Active synthesis of C24:5, n-3 fatty acid in retina. *Biochem J* 316 (Pt 3):859–864.
42. Li W, *et al.* (2007) Elovl4 haploinsufficiency does not induce early onset retinal degeneration in mice. *Vision Res* 47:714–722.
43. Raz-Prag D, *et al.* (2006) Haploinsufficiency is not the key mechanism of pathogenesis in a heterozygous Elovl4 knockout mouse model of STGD3 disease. *Invest Ophthalmol Vis Sci* 47:3603–3611.
44. Rotstein NP, Aveldano MI (1988) Synthesis of very long chain (up to 36 carbon) tetra, penta and hexaenoic fatty acids in retina. *Biochem J* 249:191–200.
45. Aveldano MI, Robinson BS, Johnson DW, Poulos A (1993) Long and very long chain polyunsaturated fatty acids of the n-6 series in rat seminiferous tubules. Active desaturation of 24:4n-6 to 24:5n-6 and concomitant formation of odd and even chain tetraenoic and pentaenoic fatty acids up to C32. *J Biol Chem* 268:11663–11669.
46. Denic V, Weissman JS (2007) A molecular caliper mechanism for determining very long-chain fatty acid length. *Cell* 130:663–677.
47. Schneiter R, *et al.* (1996) A yeast acetyl coenzyme A carboxylase mutant links very-long-chain fatty acid synthesis to the structure and function of the nuclear membrane-pore complex. *Mol Cell Biol* 16:7161–7172.
48. McMahon A, Jackson SN, Woods AS, Kedzierski W (2007) A Stargardt disease-3 mutation in the mouse Elovl4 gene causes retinal deficiency of C32–C36 acyl phosphatidylcholines. *FEBS Lett* 581:5459–5463.
49. Xiao J, Chodosh J (2005) JNK regulates MCP-1 expression in adenovirus type 19-infected human corneal fibroblasts. *Invest Ophthalmol Vis Sci* 46:3777–3782.
50. Kang ZB, *et al.* (2001) Adenoviral gene transfer of Caenorhabditis elegans n-3 fatty acid desaturase optimizes fatty acid composition in mammalian cells. *Proc Natl Acad Sci USA* 98:4050–4054.
51. Ge Y, *et al.* (2002) Gene transfer of the Caenorhabditis elegans n-3 fatty acid desaturase inhibits neuronal apoptosis. *J Neurochem* 82:1360–1366.